A Journal of the Gesellschaft Deutscher Chemiker

Angewandte International Edition GDCh Chemie

www.angewandte.org

Accepted Article

Title: A Water-soluble, NIR-absorbing Quaterrylenediimide Chromophore for Photoacoustic Imaging and Efficient Photothermal Cancer Therapy

Authors: Klaus Müllen, Chang Liu, Shaobo Zhang, Jianhao Li, Jie Wei, and Meizhen Yin

To be cited as: *Angew. Chem. Int. Ed.* 10.1002/anie.201810541
Angew. Chem. 10.1002/ange.201810541

Link to VoR: http://dx.doi.org/10.1002/anie.201810541
http://dx.doi.org/10.1002/ange.201810541

WILEY-VCH

10.1002/anie.201810541

WILEY-VCH

A Water-soluble, NIR-absorbing Quaterrylenediimide Chromophore for Photoacoustic Imaging and Efficient Photothermal Cancer Therapy

Chang Liu,[a] Shaobo Zhang,[a] Jianhao Li,[a] Jie Wei,[a] Klaus Müllen[b] and Meizhen Yin*[a]

Abstract: Precision phototheranostics, including photoacoustic imaging and photothermal therapy, requires stable photothermal agents. Developing photothermal agents with high stability and high photothermal conversion efficiency (PTCE) remains a considerable challenge in biomedical applications. Herein, we introduce a new photothermal agent based on water-soluble quaterrylenediimide (QDI) that can self-assemble into nanoparticles (QDI-NPs) in aqueous solution. Incorporation of polyethylene glycol (PEG) into the QDI core significantly enhances both physiological stability and biocompatibility of QDI-NPs. These highly photostable QDI-NPs exhibit exciting advantages including intense absorption in the near-infrared (NIR) and high PTCE of up to 64.7 ± 4%. This is higher than that of many other organic photothermal agents, such as graphene or commercial indocyanine green (ICG). Their small size of approximately 10 nm enables a sustained retention in deep tumor sites and at the same time proper clearance from the body. QDI-NPs allow high-resolution photoacoustic imaging and efficient 808 nm laser-triggered photothermal therapy of cancer *in vivo*. The current study opens a promising way for precision phototheranostics.

Phototheranostics has attracted considerable attention as a compelling platform in cancer photoacoustic imaging (PAI) and photothermal therapy (PTT).[1] Due to the deep penetration and minimal invasiveness through tissue, near-infrared (NIR, 690-900 nm) light has been considered as ideal source to trigger a photothermal effect.[2] Therefore, NIR-absorbing agents have been widely investigated in cancer phototheranostics.[3] However, the design of highly efficient photothermal agents still faces many challenges.[4] NIR-absorbing organic agents are made from extended conjugated π-systems and suffer from oxidative decomposition, resulting in photobleaching and subsequent insufficient photothermal conversion efficiency (PTCE).[5] Current inorganic photothermal agents , apart from unknown degradation pathways, raise serious biosafety concerns.[6] Therefore, it is of vital significance to develop new NIR-absorbing photothermal agents.

[a] C. Liu, S. Zhang, J. Li, Prof. J. Wei, Prof. M. Yin
Beijing Advanced Innovation Center for Soft Matter Science and Engineering, BAIC-SM, Beijing Laboratory of Biomedical Materials, Beijing University of Chemical Technology, Beijing, 100029 (China)
E-mail: yinmz@mail.buct.edu.cn

[b] Prof. K. Müllen
Max Planck Institute for Polymer Research; Institute of Physical Chemistry, Johannes Gutenberg University Mainz, Duesbergweg 10-14, Mainz, D-55128 (Germany)

Supporting information for this article is given via a link at the end of the document.

Recently, a terrylenendiimide-based photothermal agent has been investigated under 660 nm laser irradiation.[7] However, the wavelength of 660 nm defines a serious limitation for clinical applications. The core-expanded quaterrylenediimide (**QDI**)[8] possesses an intense absorption at a wavelength of 808 nm which holds a great potential for deep-tissue penetration and minimal optical interference in phototheranotics. Because of the poor water solubility brought about by its large unpolar and rigid π-system,[9] **QDI** derivatives have never been employed in phototheranostics. Herein, we exploited the NIR-absorbing, water-soluble QDI-cored star-macromolecule **P(QDI)** (Figure 1A) containing multi-poly(ethylene glycol) (PEG) chains for phototheranostics *in vivo*.

Organic molecules have been shown to assemble to nanoparticles,[10] among which ultra-small ones (about 10 nm) exhibited proper clearance from the body and thus furnished high biosecurity.[11] Further, ultra-small nanoparticles display prolonged blood circulation time together with an enhanced permeability and retention (EPR) effect, and thus lead to deep tumor permeation.[12] In this study, aiming at cancer phototheranostic applications, photostable QDI-NPs offer distinct advantages such as: i) a high PTCE of up to 64.7 ± 4%, which is higher than the values of most organic photothermal agents,[13] and also higher than that of most inorganic agents;[4,14] ii) a diameter of 10.8 ± 1.4 nm, leading to an efficient tumor-targeting, excellent metabolism, and low biotoxicity during prolonged blood circulation; iii) the incorporation of poly(ethylene glycol) (PEG), which is approved by Food and Drug Administration and greatly enhances biocompatibility of QDI-NPs. Thus, QDI-NPs can enable pthototheranostic applications including sensitive PAI and efficient PTT *in vivo*.

The **QDI** molecule was synthesized from perylene monoimide in a four-step process by bromination, Suzuki cross-coupling, and cyclodehydrogenation under basic conditions according to the literature[15] (Figure S4 in the supporting information (SI)). Subsequently, bromination of **QDI** with an excess of molecular bromine afforded the hexabrominated QDI-1 (Figure 1A). Then, phenoxylation with 4-(2-hydroxyethyl) phenol occurred at the four most reactive bromides closest to the imide positions of QDI-1, resulting in the tetra(hydroxyethylphenoxy) substituted QDI-2. QDI-2 was further subjected to fourfold esterification with carboxy-functionalized PEG_{2000} (M_{nPEG} ≈ 2000) to obtain the targeted macromolecule **P(QDI)**.

P(QDI) with a high water-solubility (>7.5 mg·mL^{-1}) self-assembled into QDI-NPs in aqueous solutions (Figure 1A). The morphology of QDI-NPs was first studied by high-resolution transmission electron microscopy (HRTEM), which exhibited well-defined spherical particles (Figure 1B). The HRTEM images provided an average diameter of the QDI-NPs as 10.8 ± 1.4 nm.

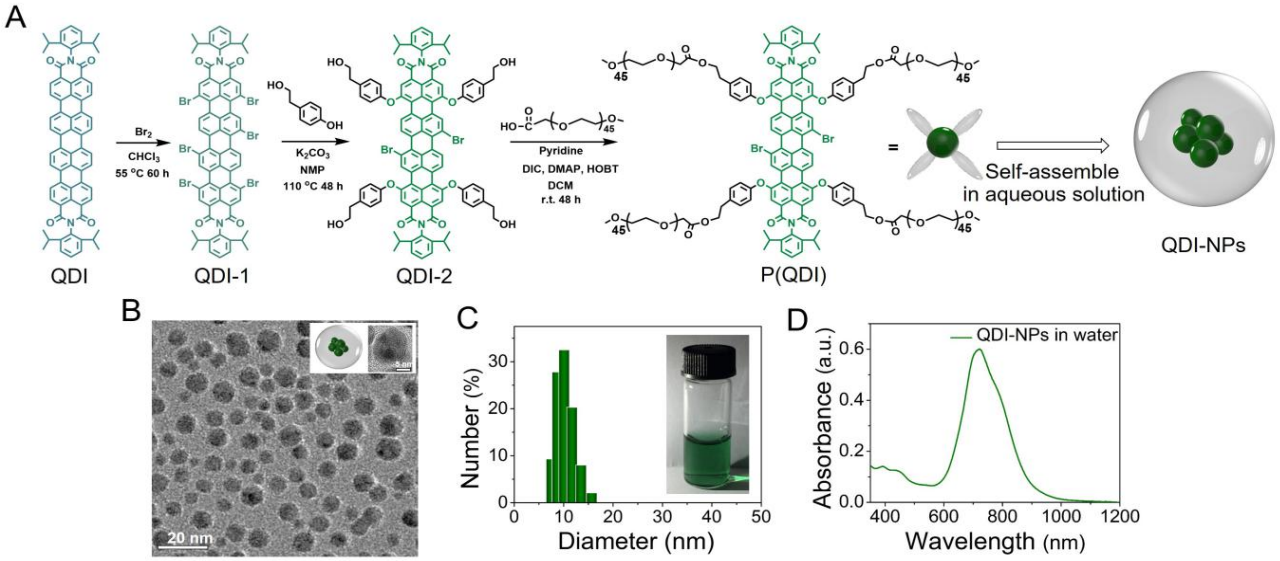

Figure 1. Preparation and characterization of QDI-NPs. (A) Synthesis of the targeted product **P(QDI)** and the self-assembly of **P(QDI)** to form QDI-NPs in aqueous solution. (B) HRTEM images of QDI-NPs. The inset shows a simulated illustration and a magnified image. (C) DLS profile of QDI-NPs. The inset presents a photograph of QDI-NPs in water. (D) Vis-NIR absorption spectrum of QDI-NPs in water.

This finding could be confirmed by dynamic light scattering (DLS) (Figure 1C). The sizes of QDI-NPs were monitored by DLS in phosphate buffered saline (PBS) and deionized water, respectively. No obvious changes in their size and precipitation behavior were observed in both solutions after storage at 4 °C for two weeks, confirming the good chemical and physiological stability of QDI-NPs in aqueous solutions (Figure S6). This is essential forreducing risks of adverse effects *in vivo*. The absorption spectrum of QDI-NPs in water (Figure 1D) revealed a high molar extinction coefficient (about $1.3*10^5$ $M^{-1}\cdot cm^{-1}$) suggesting a pronounced capability to absorb light energy in NIR.

Weak fluorescence emission at 830 nm and low reactive oxygen species generation of QDI-NPs were detected after excitation (Figure S7 and S8) which suggested that vibrational relaxation may play a major role thus furnishing a useful photothermal effect. This was tested under NIR laser (808 nm) irradiation. The solution temperature of QDI-NPs at different concentrations regularly increased under irradiation as recorded by thermal images. A high value of 61.7 °C could be recorded in 300 s (Figure 2A and 2B). Furthermore, the solution of QDI-NPs at a given concentration (150 $\mu g\cdot mL^{-1}$) was irradiated at different laser power densities (0.1~1 $W\cdot cm^{-2}$) revealing significant temperature increases (Figure S9). Moreover, a steady-state temperature was recorded through the heating and cooling profiles (Figure S10). The PTCE (η) of the QDI-NPs was calculated to be 64.7 ± 4% which is higher than the values of most reported organic photothermal agents.[13] The high PTCE value of QDI-NPs may be attributed to their tight π-π interactions thus favoring energy relaxation in nanostructures.[16] Besides, QDI-NPs maintained an undiminished ability of heating, unchanged absorption and nanosize after cyclic laser irradiation (Figure S11) indicating their excellent photostability in water. Both the strong photothermal effect and excellent photostability highlight the potential of QDI-NPs for PTT.

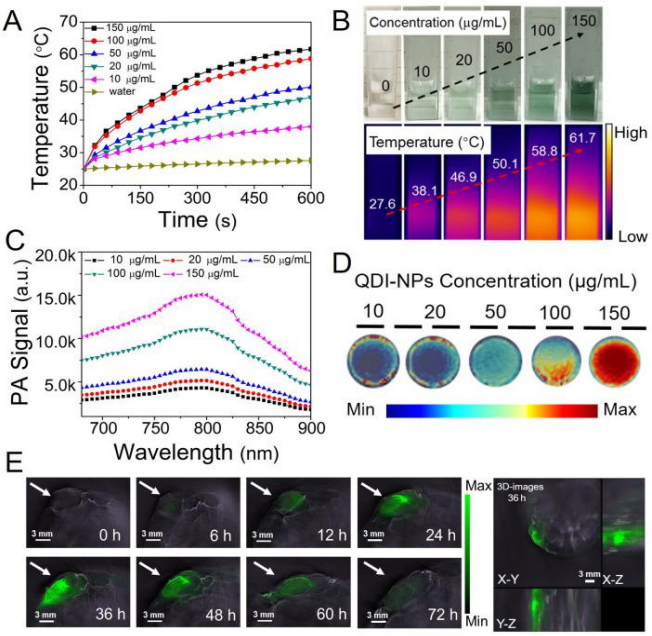

Figure 2. Photothermal and photoacoustic properties of QDI-NPs. (A) Temperature curves of QDI-NPs in PBS solutions at different concentrations. (B) Optical photographs and thermal images of QDI-NPs in PBS solutions after laser irradiation. (C) Photoacoustic spectra of QDI-NPs in PBS solutions. (D) Photoacoustic images of QDI-NPs as a function of the concentration in a normalized phantom mold. (E) *In vivo* photoacoustic images of tumor tissue (arrows) at different times (left) and the 3D-images (right) at 36 h after the intravenous injection of QDI-NPs. Scale bars: 3 mm.

Our QDI-NPs were then employed for photoacoustic diagnosis and visualization of cancer. The photoacoustic spectra of QDI-NPs were plotted in a normalized phantom mold (Figure 2C). The detected photoacoustic intensities at 800 nm indicate superior photoacoustic (NIR) properties of QDI-NPs in aqueous phase (Figure 2D). A linear relationship between the concentrations and the mean photoacoustic signals (R^2 = 0.985)

was calculated (Figure S12). The positive photoacoustic property in phantom motivated us to explore the PAI *in vivo*, aiming to visualize the location, shape, and size of solid tumors. Thus, we inspected PAI in 4T1 (murine breast cancer) tumor-bearing BALB/c mice, and the high-resolution photoacoustic images were recorded in a time-dependent protocol after intravenous injection of QDI-NPs (Figure 2E, left). The results revealed that QDI-NPs passively permeated into the deep tumor region and reached the highest accumulation at approximately 36 h post-injection during a blood circulation time. The 3D images of the tumor at 36 h further verified the precision PAI capability of QDI-NPs (Figure 2E, right). The photoacoustic intensities of QDI-NPs in the tumor region were determined (Figure S13). Taking advantage of the intrinsic photothermal effect, the QDI-NPs can be used as photoacoustic contrast agents for an efficient visualization of cancer *in vivo*.

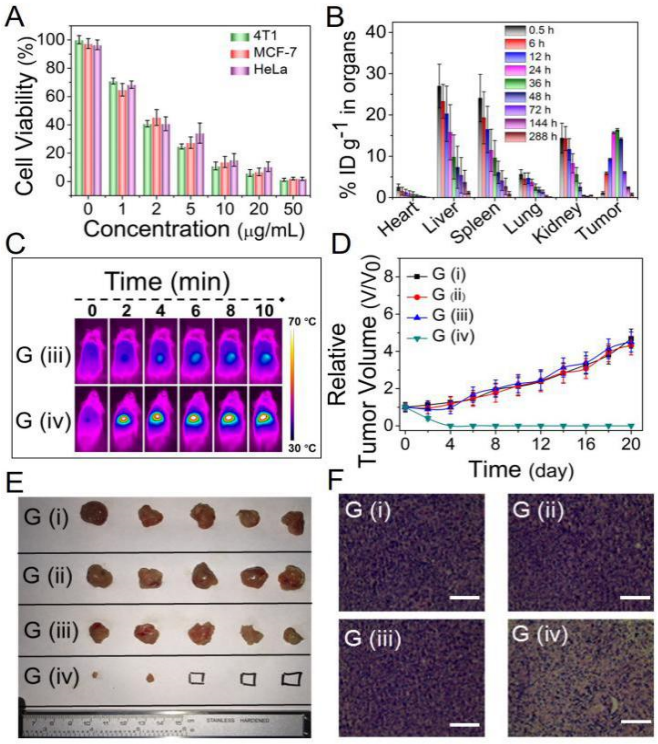

Figure 3. The pharmacokinetics of QDI-NPs, and PTT *in vitro* and *in vivo*. (A) Relative viability of 4T1 cells, MCF-7 cells and HeLa cells co-incubated with different concentrations of QDI-NPs for 24 h. Cells treated with PBS combined with laser irradiation were used as controls. (B) Tissue distribution of QDI-NPs in mice determined by the concentration in each organ. (C) Thermal images of 4T1 tumor-bearing mice during the therapeutic process. (D) Tumor volume growth curves of tumors in different groups after laser irradiation. (E) Photos of stark tumors collected from the mice in different groups at the end of PTT. (F) The H&E-stained images of tumor after PTT. 808 nm laser irradiation was at 1 W·cm^{-2} for 10 min. Error bars, mean ± SD (two-tailed Student's test), Scale bar: 100 μm.

Photothermal agents must possess low cytotoxicity in dark and efficient PTT against cancer cells under light irradiation. The potential cytotoxicity of the QDI-NPs was investigated by a standard cell counting kit-8 (CCK-8) assay in three cancer cell lines: 4T1 cells, human breast cancer (MCF-7) cells, human cervical carcinoma (HeLa) cells and two non-cancer cell lines: L929 cells, rat bone marrow stromal (BMSC) cells. No cytotoxicity was detected after co-incubation with high-concentration (1000 μg·mL^{-1}) solutions of QDI-NPs for 24 h and prolonged 48 h (Figure S14). These results imply that the QDI-NPs display no cytotoxicity and thus hold promise in PTT applications. Under laser irradiation for 5 min (808 nm, 1 W·cm^{-2}), the viability of cancer cells decreased with the increase of QDI-NPs concentration. A quite low IC50 of 1.7 μg·mL^{-1} demonstrated an efficient PTT of QDI-NPs (Figure 3A). Live/dead staining further supported the PTT results *in vitro* (Figure S15), in which live and dead 4T1 cells were differentiated by co-staining with PI (red fluorescence; dead cells) and calcein AM (green fluorescence; living cells) after the same laser irradiation. Almost all the cells were positive for red fluorescence after combination of the QDI-NPs and laser irradiation, thus indicating the cancer cell extinction. The superior biocompatibility and efficient PTT again characterize QDI-NPs as remarkable photothermal agents.

The pharmacokinetics and pharmacodynamics of QDI-NPs were checked in 4T1 tumor-bearing mice. After intravenous (i.v.) injection of QDI-NPs (5 mg·kg^{-1}), tissue distribution studies demonstrated that the highest concentrations of QDI-NPs were detected during 24~48 h in the tumor region, suggesting high tumor accumulation (Figure 3B). QDI-NPs were mainly taken up by liver and spleen, but were barely cleared through urinary excretion due to the size of QDI-NPs above the kidney filtration threshold (ca. 5.5 nm)[17] (Figure S16).The remaining concentrations of QDI-NPs in each organ were quite low at 288 h post-injection, indicating that QDI-NPs can be properly cleared from the body.

To investigate the PTT of cancer *in vivo*, four groups were randomly established from 4T1 tumor-bearing mice, as follows: G (i) PBS administration (i.v. injection), G (ii) only QDI-NPs administration (i.v. injection, 5 mg·kg^{-1}), G (iii) only laser irradiation administration (808 nm, 1 W·cm^{-2}, 10 min), and G (iv) QDI-NPs administration (i.v. injection, 5 mg·kg^{-1}) combined with laser irradiation. We established the 36 h post-injection as the optimum treatment time, according to the accumulation concentration detection of QDI-NPs in the tumor region (Figure 3B). At 36 h post-injection, the mice from G (iii) and G (iv) were dealt with laser irradiation. The mice of G (iv) displayed a rapid temperature increase to 69.7 °C. In the control group of G (iii), the temperature increased to 41.1 °C under the same irradiation condition without QDI-NPs (Figure S17). A thermal imaging camera recorded the treating process every two minutes, indicating that the QDI-NPs could efficiently induce a temperature increase for PTT of cancer *in vivo* (Figure 3C). During the subsequent 20-day observation period the tumor volumes of the four groups were recorded every other day (Figure 3D). There was no tumor outburst after initial elimination in G (iv). In contrast, the tumors from the other three groups showed consistently high growth rates, suggesting that the PTT induced by QDI-NPs can significantly eliminate the cancer (Figure S18). The anatomized tumor displayed eradication and the lowest values in size and weight in group (iv) than those in the other three groups (Figure 3E and S19). The bioactivity of residual tumor tissues was further verified through a pathological examination by hematoxylin and eosin (H&E) staining (Figure 3F). High extermination of malignant cells was observed from G (iv), including cell shrinkage, separation and fragmentized nuclei. Importantly, during the 20-day observation period, there were no abnormalities of the treated mice in the daily behaviors and the monitored body weight values were steady (Figure S20), thus, suggesting the QDI-NPs displayed no adverse effects during PTT *in vivo*. Altogether, the QDI-NPs can passively accumulate

in the tumor region and successfully exterminate the tumor tissue through PTT *in vivo*.

Finally, the biosecurity of QDI-NPs was thoroughly verified in healthy mice. A further aspect is the ultra-small size of the QDI-NPs which renders them potential candidates for biomedical applications owing to proper clearance from the body and minimum long-term biotoxicity. The blood circulation and tissue bio-distribution were studied through measuring the concentrations of QDI-NPs (Figure S21). The results, as well as the photoacoustic intensity of major organs (Figure S22), confirmed the excellent metabolism of QDI-NPs in the body. Further, the blood circulation and tissue distribution failed to show any influence of QDI-NPs on the body. We determined the long-term toxicity of QDI-NPs in major organs after intravenous injection (45 mg·kg-1) in healthy mice. At 30 day post-injection, the major organs were harvested from the mice treated with QDI-NPs and PBS as a control, respectively. The histopathological studies through the H&E staining method revealed no noticeable damage or inflammation in the organs from both groups (Figure S23). In addition, the analysis of blood biochemistry confirmed that the liver and kidney functions were not affected by QDI-NPs (Figure S24). One concludes that the ultra-small QDI-NPs reveal a proper clearance from the body without biotoxicity *in vivo*.

In summary, we demonstrated a strong photothermal effect for the QDI-cored star-macromolecule **P(QDI)** with multi-PEG chains for phototheranostic applications. **P(QDI)** shows strong NIR absorption and can assemble into QDI-NPs with ultra-small size of approximately 10 nm in aqueous solutions. With their excellent stability against periodic laser-irradiation, the assembled QDI-NPs exhibit a high and stable PTCE of up to 64.7 ± 4%, thus qualifying them as promising photothermal agents for cancer therapy. The QDI-NPs could efficiently passively target tumors and visualize the tumor outline with high spatial resolution *in vivo*. Consequently, the systematic PTT of cancer was successfully implemented *in vitro* and *in vivo*. Most importantly, QDI-NPs present proper clearance from the body without biotoxicity according to pharmacokinetic studies in healthy mice. This investigation provides firm evidence that the hydrophobic QDI molecule can be applied as a biomedical photothermal agent after appropriate chemical modification. These NIR-absorbing QDI-NPs, as stable and powerful photothermal species, appear to enrich the toolbox of phototheranostics and to act as useful therapeutic systems in future biomedical applications.

Acknowledgements

The National Natural Science Foundation of China (21774007, 21574009, 51873009 and 51573012), Fundamental Research Funds for the Central Universities (PT1811), Beihuazhongri United Fund (PYBZ1822), and the Max-Planck-Society are acknowledged for financial support and the Joannes-Gutenberg University for a scholarship from the Gutenberg Research College.

Conflict of interest

The authors declare no conflict of interest.

Keywords: NIR-absorption • quaterrylenediimide • photoacoustic imaging • photothermal conversion efficiency • pharmacokinetics

[1] a) K. K. Ng, G. Zheng, *Chem. Rev.* **2015**, *115*, 11012-11042; b) L. Cheng, C. Wang, L. Feng, K. Yang, Z. Liu, *Chem. Rev.* **2014**, *114*, 10869-10939; c) D. Y. Lee, J. Y. Kim, Y. Lee, S. Lee, W Miao, H. S. Kim, J.-J. Min, S. Jon, *Angewandte Chemie,* **2017**, *129*, 13872-13876; *Angew. Chem. Int. Ed.* **2017**, *56*, 13684-13688; d) L. Du, H. Qin, T. Ma, T. Zhang, D. Xing, *ACS Nano*, **2017**,*11*, 8930–8943.

[2] a) R. Weissleder, *Nat. Rev. Cancer.* **2002**, *2*, 11-18; b) B. Shi, K. Jie, Y. Zhou, J. Zhou, D. Xia, F. Huang, *J. Am. Chem. Soc.* **2015**, *138*, 80-83.

[3] a) X. Huang, I. H. El-Sayed, W. Qian, M. A. El-Sayed, *J. Am. Chem. Soc.* **2006**, *128*, 2115-2120; b) C. Liang, S. Diao, C. Wang, H. Gong, T. Liu, G. Hong, X. Shi, H. Dai, Z. Liu, *Adv. Mater.* **2014**, *26*, 5646-5652. c) X. Song, H. Gong, T. Liu, L. Cheng, C. Wang, X. Sun, C. Liang, Z. Liu, *Small* **2014**, *10*, 4362-4370.

[4] a) Q. Dong, X. Wang, X. Hu, L. Xiao, L. Zhang, L. Song, M. Xu, Y. Zou, L. Chen, Z. Chen, W. Tan, *Angew. Chem.* **2018**, *130*, 183-187; *Angew. Chem. Int. Ed.* **2018**, *57*, 177-181; b) D. Y. Lee, J. Y. Kim, Y. Lee, S. Lee, W. Miao, H. S. Kim, J. J. Min, S. Jon, *Angew. Chem.* **2017**, *129*, 13872-13876; *Angew. Chem. Int. Ed.* **2017**, *56*, 13684-13688.

[5] a) L. L. Lock, C. D. Reyes, P. Zhang, H. Cui, *J. Am. Chem. Soc.* **2016**, *138*, 3533-3540; b) *Prog. Polym. Sci.*, **2015**, *46*, 25-54; c) G. Wei, Z. Su, N. P. Reynolds, P. Arosio, I. W. Hamley, E. Gazit, R. Mezzenga, *Chem. Soc. Rev.* **2017**, *46*, 4661-4708.

[6] Q. Zou, M. Abbas, L. Zhao, S. Li, G. Shen, X. Yan, *J. Am. Chem.Soc.* **2017**, *139*, 1921-1927.

[7] a) S. Zhang, W. Guo, J. Wei, C. Li, X. J. Liang, M. Yin, *ACS Nano*, 2017, 11, 3797-3805; b) S. Zhang, J. Li, J. Wei, M. Yin, *Sci. Bull.* **2018**, *63*, 101-107.

[8] G. Yang, D. Yang, P. Yang, R. Lv, C. Li, C. Zhong, F. He, S. Gai, J. Lin, *Chem. Mater.* **2015**, *27*, 7957-7968.

[9] L. Chen, C. Li, K. Müllen, *J. Mater. Chem. C* **2014**, *2*, 1938-1956.

[10] a) Y. Zheng, S. You, C. Ji, M. Yin, W. Yang, J. Shen, *Adv. Mater.*, **2016**, *28*, 1375-1380; b) W. Cheng, H. Cheng, S. Wan, X. Zhang, M. Yin, *Chem. Mater.*, **2017**, *29*, 4218-4226; c) H. Xia, H. Fu, Y. Zhang, K. C. Shih, Y. Ren, M. Anuganti, M. Nieh, J. Cheng, Y. Lin, *J. Am. Chem. Soc.* **2017**, *139*, 11106-11116;

[11] a) R. A. Petros, J. M. DeSimone, *Nat. Rev. Drug Discov.* **2010**, *9*, 615-627; b) M. Elsabahy, K. L. Wooley, *Chem. Soc. Rev.* **2012**, *41*, 2545-2561.

[12] a) C. Ji, Q. Gao, X. Dong, W. Yin, Z. Gu, Z. Gan, Y. Zhao, M. Yin, *Angew. Chem.* **2018**, *130*, 11554-11558; *Angew. Chem. Int. Ed.*, **2018**, *57*, 11384-11388; b) Y. Zhang, W. Chen, C. Yang, Q. Fan, W. Wu, X. Jiang, *J. Contr. Rel.* **2016**, *237*, 115-124; c) V. P. Chauhan, T. Stylianopoulos, J. D. Martin, Z. Popović, O. Chen, W. S. Kamoun, M. G. Bawendi, D. Fukumura, R. K. Jain, *Nat. Nanotechnol.* **2012**, 7, 383-388; d) H. Su, J. M. Koo, H. Cui, *J. Contr. Rel.* **2015**, *219*, 383-395.

[13] a) Y. Cai, P. Liang, Q. Tang, X. Yang, W. Si, W. Huang, Q. Zhang, X. Dong, *ACS Nano* **2017**, *11*, 1054-1063; b) Y. Lyu, D. Cui, H. Sun, Y. Miao, H. Duan, K. Pu, *Angew. Chem.* **2017**, *129,* 9283-9287; *Angew. Chem. Int. Ed.* **2017**, *56*, 9155-9159; c) Q. Zou, M. Abbas, L. Zhao, S. Li, G. Shen, X. Yan, *J. Am. Chem. Soc.* **2017**, *139*, 1921-1927.

[14] a) G. Lv, W. Guo, W. Zhang, T. Zhang, S. Li, S. Chen, A. S. Eltahan, D. Wang, Y. Wang, J. Zhang, *ACS Nano* **2016**, *10*, 9637-9645; b) W. Tao, X. Ji, X. Xu, M. A. Islam, Z. Li, S. Chen, P. E. Saw, H. Zhang, Z. Bharwani, Z. Guo, J. Shi, O. C. Farokhzad, *Angew. Chem.* **2017**, *129*, 12058-12062; *Angew. Chem. Int. Ed.* **2017**, *56*, 11896-11900.

[15] a) H. Quante,; K. Müllen, *Angew. Chem.* **1995**, *107*, 1487-1489; *Angew. Chem. Int. Ed.* **1995**, *34*, 1323-1325; b) Y. Avlasevich, S. Müller, P. Erk, K. Müllen, *Chem. Eur. J.* **2007**, *13*, 6555-6561.

[16] F. Nolde, W. Pisula, S. Müller, C. Kohl, K. Müllen, *Chem. Mater.* **2006**, *18*, 3715-3725.

[17] H. S. Choi, W. Liu, P. Misra, E. Tanaka, J. P. Zimmer, B. Itty Ipe, M. G. Bawendi, J. V. Frangioni, *Nat. Biotechnol.* **2007**, *25*, 1165-1170.

COMMUNICATION

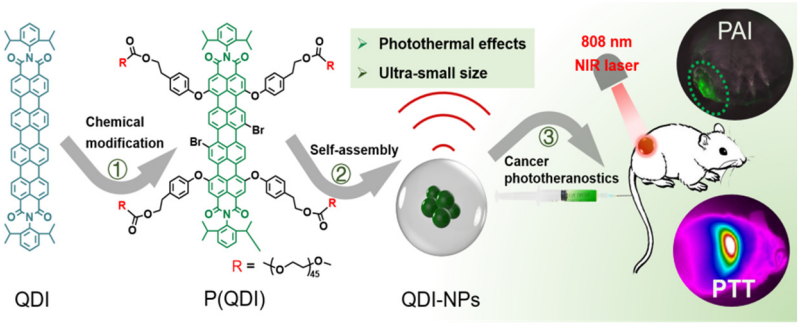

*C. Liu, S. Zhang, J. Li, J. Wei, K. Müllen, M. Yin**

Page No. – Page No.

Title: A Water-soluble, NIR-absorbing Quaterrylenediimide Chromophore for Photoacoustic Imaging and Efficient Photothermal Cancer Therapy

Entry for the Table of Contents

Text for Table of Contents:

A water-soluble NIR-absorbing photothermal agent for phototheranostics has been developed based on quaterrylenediimide (QDI). The poly(ethylene glycol)-functionalized QDI can self-assemble into QDI-nanoparticles (QDI-NPs) with sizes of approximate 10 nm in aqueous solution. QDI-NPs exhibit high-resolution photoacoustic imaging and efficient photothermal cancer therapy at 808 nm NIR laser irradiation.